International Journal of Computational and Experimental Science and ENgineering (IJCESEN)

Vol. 11-No.1 (2025) pp. 1553-1566
http://www.ijcesen.com

ISSN: 2149-9144

Research Article

Numerical Modeling-Based Comparison of Leap-Frog and Implicit Crank-Nicolson Schemes for Instantaneous Spill of Pollutant in Rivers

Fatima M.A. Al-khafaji[1], Hussein A. M. Al-Zubaidi[2]*

[1]Department of Environmental Engineering, College of Engineering, University of Babylon, Babylon, Iraq
* **Corresponding Author Email:** alkhafajif541@gmail.com - **ORCID:** 0009-0008-0616-9604

[2]Department of Environmental Engineering, College of Engineering, University of Babylon, Babylon, Iraq
* **Corresponding Author Email:** hussein.alzubaidi@uobabylon.edu.iq ; alzubaidih10@gmail.com - **ORCID:** 0000-0001-8746-8543

Article Info:

DOI: 10.22399/ijcesen.1190
Received : 17 January 2025
Accepted : 13 March 2025

Keywords :

Advection Dispersion Equation,
Instantaneous Spills,
Crank-Nicolson Scheme,
Leap-Frog Scheme,
Numerical Methods,
Pollutants Transport.

Abstract:

Numerical modeling of pollutant spills that are released instantaneously in rivers has been commonly applied for water quality purposes. Recently, different numerical schemes have been used to solve for the river hydrodynamics from the shallow water equations (SWEs), affecting the longitudinal pollutant concentrations prediction of the advection-dispersion equation (ADE). In this study, two numerical schemes for solving the SWEs, Explicit Leap-Frog Scheme (ELFs) and Implicit Crank-Nicolson Scheme (ICNs), were implemented based on a field case study, and the pollutant concentrations distribution along the river were explored and compared to the ADE analytical solution. Results showed that the maximum concentration predicted by the ICNs decreased from 0.1071 to 0.0084 ppm after 5 and 8 days from the spill date, respectively, with an average flow velocity of 0.1545 m/sec. On the other hand, the maximum concentration predicted by the ELFs decreased from 0.1068 to 0.0083 ppm during the same period with an average flow velocity of 0.1550 m/sec. Accordingly. both schemes revealed good agreement compared to the analytical solution, for instance, at the simulation time of 8 days the ICNs statistical errors were RMSE of 0.000174 ppm and MAE of 0.0000771 ppm, while the ELFs errors were RMSE of 0.000182 ppm and MAE of 0.0000824 ppm. In terms of computational time, the ICNs spent higher cost of about 0.5982 sec during the simulation period of 8 days, while the ELFs took about 0.1738 sec for the same period. Furthermore, for both schemes as the longitudinal increments value of the finite difference grid increases, the model time step increases and the execution time decreases. Thus, it is necessary to choose time step and spatial increment length that obey the governing equation stability condition in order to conserve the concentrations distribution along the river spatially and temporally and make good predictions.

1. Introduction

The numerical prediction of instantaneous spills release in rivers is one of the areas that provide support for water quality management processes [1-57]. Spills may be (oils, fuel, chemicals, wastewater or any other mass). These spills result from (ship collision, shipping, storage, ship cleaning, tearing and leaking of pipelines and other accidents). When pollutants are spilled at a release site, the pollutant spill is highly concentrated and appears as a small plume in the water. When a pollutant moves downstream through advection, it also spreads through the river. Due to diffusion, the plume becomes larger and contains the highest concentration of pollutants in the plume center and decreases towards its borders under the traditional Fickian dispersion theory. Measurements of concentration in space at a given time result in a graph similar to the Gaussian distribution curve [22]. Hence, the flow velocity and water depth are important hydraulic parameters in the pollutant transport process [26]. Accordingly, reliable methods must be developed to predict the transport of instantaneous spills in rivers in order to prevent large-scale spills and disasters [16,58].

Since the instantaneous spills can transport for long distance along the river length with various risk ranges, a crucial modeling technique for simulating the dispersion of pollutants is solving the ADE.

One of the efficient numerical solution methods is by finite differences. Different models have been developed with various numerical approaches to predict the pollutant concentrations over distance and time. Depending on the developed model complexity, different accuracy scores have been achieved compared to the exact pollutant concentrations distribution, which is Gaussian distribution. For instance, Yip et al. (2021) solved the one dimensional advection-dispersion equation (ADE) numerically to model an ideal instantaneous pollutant releases of pollutants inside a 2.5 m narrow straight channel of constant longitudinal velocity (0.00083 m/sec) [56]. The numerical solution was performed explicitly using the upwind scheme for the advection term and the 2^{nd}-order central difference for the dispersion term. To verify the validity of the model, it was compared with the analytical solution, taking into account the factors affecting the transport of pollutants such as the diffusion coefficient and longitudinal velocity. This simple model case required a very low time step (0.001 min) to simulate 313 spatial nodes in order to achieve the numerical stability and get the best agreement with the analytical solution (a symmetrical bell shaped distribution). The spill can transport longitudinally in rives for long distance downstream depending on the substance decay rate, dispersion coefficient, and longitudinal velocity. Hence, adding the decay rate to the ADE in addition to spatial and temporal variability of longitudinal velocity must be considered in real case studies associated to river systems. Regarding the diffusivity influence on the bell shaped distribution, Peruzzi et al. (2021) [29] conducted a field tracer study to measure the longitudinal dispersion coefficient in typical rural channels to understand the most appropriate longitudinal dispersion coefficient empirical formulas when implementing one-dimensional models [29]. The plume concentrations of the injected sodium chloride were compared to the ADE analytical solution temporally and spatially, producing less than 8% difference between the maximum concentrations with less than 0.0044 Kg/m^3 root mean squared error. In addition, skewed theoretical Gaussian distribution generated at a fixed location over time with 0.0026 Kg/m^3 root mean squared error. The results also showed that the greater the dispersion coefficient, distance, and time, the lower the concentration. Even though the ADE exact solution is a perfect bell shape, the concentration field distribution was shifted to the left or right, following the exact solution of Gaussian distribution shape. Similarly, various models have been developed with different numerical schemes to solve the ADE in the context of pollutant transport in rivers. For example, [4] and [39] employed the explicit Crank-Nicolson finite difference scheme in the solution method. A comparison between analytical and numerical solutions was conducted to validate the accuracy of the numerical model. Their results demonstrated that the numerical model is highly accurate, with a very low error percentage compared to the analytical solution. Additionally, it was emphasized that a very small spatial step is crucial to ensure the stability of the model and to yield precise results. Various values were considered for diffusion coefficient, velocity, and time, revealing that as these parameters increased, the concentration of pollutants decreased. Furthermore, an increase in velocity resulted in a greater distance over which the pollutant spreads.

To be more realistic, it is important to account for the river hydrodynamic variability over time and space in the ADE solution such as flow velocity and water surface height [40,45]. In river systems, the longitudinal length scale is much larger the other dimensions' scale in which the water depth is much smaller than the wave length; therefore, the widely applicable hydrodynamic governing equations are the Shallow-Water Equations (SWEs), also known as Saint-Venant Equations [39,38,40,47,52]. Various efficient numerical schemes are greatly significant in solving the SWEs. In [32], the SWEs were linked to the ADE numerically to predict the concentration of pollutants along a channel of 30 m long during a simulation period of 30 sec. The numerical Lax-Friedrich scheme was implemented to simulate the water depth and velocity in conjunction with the Explicit Forward in Time and Central Differences in Space for first and second derivatives of the ADE numerical solution (EFTCS) to simulate the pollutant distribution. As a result, the concentration of pollutants moves downstream with time, and the mass of the pollutant decreases as time increases. Commonly, the Explicit Leap-Frog scheme (ELFs) and Implicit Crank-Nicolson scheme (ICNs) are popular numerical schemes for solving the SWEs efficiently [48]. It was used the ELFs to solve the SWEs and studied the influence of Courant Number (Cr) on the numerical solution stability [43]. The stability analysis of the scheme showed that the SWEs can become weakly unstable at a Cr value of 0.5, confirming the findings of [14]. Hence, it is required that a Cr value of less than 0.5 exists for the ELFs stability. Regarding the ICN scheme, [31] employed the ICNs for the SWEs and EFTCS for ADE simultaneously to model the water quality parameters in streams. In this model, the UPWIND scheme was used to discretize the ADE advection term. It was found that determining the velocity profile and water level by the SWEs finite difference methods were effective in providing information on pollutant concentrations, emphasizing the real-world applications capability of the ADE explicit numerical solutions.

In this analysis, two numerical schemes (explicit Leap-Frog scheme and implicit Crank-Nicolson scheme) were implemented in the SWEs numerical computations to be linked to the ADE numerical solution of the instantaneous spills release in rivers. Thus, the numerical comparisons will determine the main differences between the numerical schemes' influences on the pollutant distribution for long distances and times along the river stream. Consequently, the model sensitively to change numerical parameters such as space and time increments will be highlighted under the influence of both numerical schemes.

2. Materials and methods

Figure 1 shows a conceptual framework for studying the numerical performance evaluation applied in this study. In order to obtain the river longitudinal velocity (u) and the propagating water surface wave height (d) along the river length, the Explicit Leap-Frog and Implicit Crank-Nicolson schemes (ELFs and ICNs) were implemented to solve the SWEs. The pollutant concentration (c) is then determined longitudinally and temporally by solving the ADE analytically and numerically. Until the best calibrated and validated results of less statistical errors are obtained, the solutions of both ADE and SWEs are repeated simultaneously over the simulation period (t).

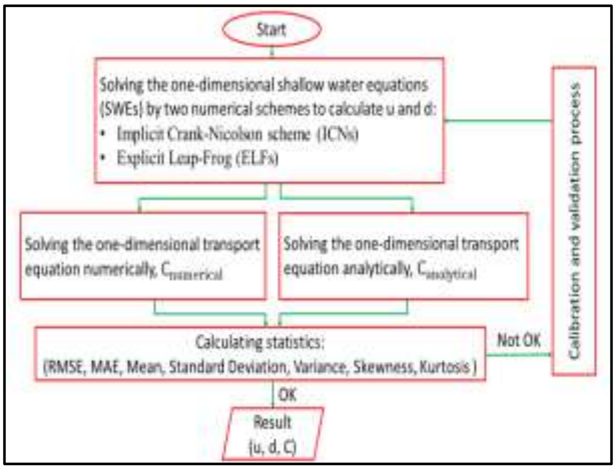

Figure 1. *Conceptual framework of the study.*

2.1 Hydrodynamics and Water Quality Transport Equations

Three governing equations were used to build a one-dimensional numerical model to simulate the instantaneous spills release in rivers. The Shallow-Water Equations (SWEs) are derived from the Navier Stokes equations to be the two fundamental hydrodynamic governing equations of continuity (Eq. 1) and momentum (Eq. 2). The water quality transport is governed by the advection-dispersion equation (ADE) to be the third governing equation (Eq. 3) [12,50]:

$$\frac{\partial d}{\partial t} + D\frac{\partial u}{\partial x} = 0 \qquad (1)$$

$$\frac{\partial u}{\partial t} + G\frac{\partial d}{\partial t} + \frac{cf.u|u|}{D} = 0 \qquad (2)$$

$$\frac{\partial C}{\partial t} + \frac{1}{A}\frac{\partial uAC}{\partial x} = \frac{E}{A}\frac{\partial^2 AC}{\partial x^2} - KC \qquad (3)$$

Where D is the river water depth at any distance along the river length (m) in which $D = d' \pm d$, d' is the initial river water height (m), d is the fluctuating wave height at the river water surface at any distance along the river length (m), u is the river average longitudinal velocity (m/sec), G is the acceleration of gravity (m/sec^2), cf is the coefficient friction and can be calculated from Chezy, Manning, or Darcy–Weisbach equations [1,27,53], C is the cross-sectional average concentration (ppm), E is the longitudinal dispersion coefficient, m^2/sec, A is the river cross section area (m^2), K is the chemical degradation rate (1/sec) and t is the time.

Hydrodynamic Governing Equations Solutions

The ELFs and ICNs were used in the finite difference discretization to solve the SWEs equations (Eq. 1 and 2) based on an equally spacing grid distribution as in Figure 2, where j and i are counters for the space and time, respectively.

The ELFs is based on the idea of jumping two time increments through the time scale domain [24,38]. (Eq. 4 and 5) and (Eq.6 and 7) display the finite difference approximations of the continuity and momentum equation, respectively, by implementing the ELFs with longitudinal distance increment of Δx and temporal increment of Δt. Solving these finite differences equation gives (d and u) at the next time level (i+1 and i+2, respectively). Hence, the numerical stability restriction for this scheme needs $Cr = u\Delta t/\Delta x < 0.5$ [17,25,43].

$$\frac{d_j^{i+1} - d_j^{i-1}}{2\Delta t} + D^i\frac{u_{j+1}^i - u_{j-1}^i}{2\Delta x} = 0 \qquad (4)$$

$$d_j^{i+1} = d_j^{i-1} - D^i\frac{\Delta t}{\Delta x}\left(u_{j+1}^i - u_{j-1}^i\right) \qquad (5)$$

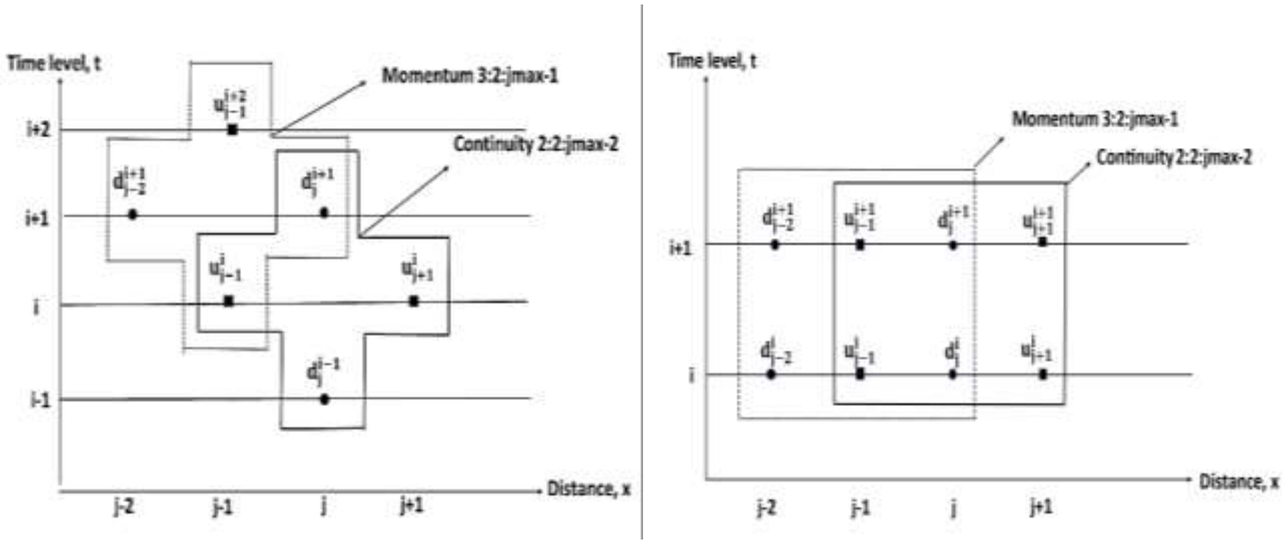

(a) (b)

Figure 2. *Grid discretization for (a) ELFs (b) ICNs.*

$$\frac{u_{j-1}^{i+2}-u_{j-1}^{i}}{2\Delta t}+G\frac{d_{j}^{i+1}-d_{j-2}^{i+1}}{2\Delta x}+\frac{1}{2}\frac{cf.\left|u^{i}\right|}{D^{i}}\left(u_{j-1}^{i+2}+u_{j-1}^{i}\right)=0 \quad (6)$$

$$u_{j-1}^{i+2}=\frac{\left(-\Delta t\frac{cf.\left|u^{i}\right|}{D^{i}}u_{j-1}^{i}-G\frac{\Delta t}{\Delta x}\left(d_{j}^{i+1}-d_{j-2}^{i+1}\right)\right)}{\left(1+\Delta t\frac{cf.\left|u^{i}\right|}{D^{i}}\right)} \quad (7)$$

Regarding the ICNs, the characterization is relatively easy to code for both linear and nonlinear problems [20]. Its implementation to the SWEs are as shown in Eq. 8 and 9 to be solved for the hydrodynamic variables at the next time level (i+1) ([23]; [58]), in which the solution is semi-implicit when β is between 0 and 1, the solution is fully explicit when $\beta=0$, and the solution is fully implicit when $\beta=1$. Using the implicit β values leads to a system of linear algebraic equations to be solved by using Thomas algorithm method for each longitudinal row of unknown nodes in the domain to calculate u and d along the x-direction [2,15]. To maintain a stable solution for the ICNs, the time step was chosen based on the Courant-Friedrichs-Lewy (CFL) condition, $Cr_g = \sqrt{gD}\Delta t/\Delta x < 1$, [11].

$$\frac{d_{j}^{i+1}-d_{j}^{i}}{\Delta t}+\square D^{i}\frac{u_{j+1}^{i+1}-u_{j-1}^{i+1}}{2\Delta x}+(1-\beta)D^{i}\frac{u_{j+1}^{i}-u_{j-1}^{i}}{2\Delta x}=0 \quad (8)$$

$$\frac{u_{j-1}^{i+1}-u_{j-1}^{i}}{\Delta t}+G\beta\frac{d_{j}^{i+1}-d_{j-1}^{i+1}}{2\Delta x}+G(1-\beta)\frac{d_{j}^{i}-d_{j-1}^{i}}{2\Delta x}+\frac{cf\left|u^{i}\right|}{D^{i}}\left(\beta u_{j-1}^{i+1}+(1-\beta)u_{j-1}^{i}\right)=0 \quad (9)$$

Water Quality Transport Equation Solutions

The ADE (Eq. 3) was solved explicitly by using the EFTCS along with UPWIND scheme for the advective term as shown in Eq. 10 and 11. The explicit solution assumes that all spatial terms in addition to the sources and sinks term are known from the current time level (i) and it has to solve for the dependent variable at next time level (i+1). As a result, it is simpler and involves less computations cost. For the numerical stability purposes, this solution is only stable when $E\Delta t/\Delta x^2 \leq 0.5$ [6,52,56,30,41,28,32,33,13].

$$C_{j}^{i+1}=C^{i}-\Delta t[UPWIND]+\frac{E\Delta t}{\Delta x^{2}A_{j}^{i}}\left[A_{i+\frac{1}{2}}^{i}\left(C_{j+1}^{i}-C_{j}^{i}\right)-A_{i-\frac{1}{2}}^{i}\left(C_{j}^{i}-C_{i-\frac{1}{2}}^{i}\right)\right]-KC_{j}^{i}\Delta t \quad (10)$$

$$UPWIND=\begin{Bmatrix}\left(uAC\,\big|_{j}^{i}-uAC\,\big|_{j-1}^{i}\right)/\left(A_{j}^{i}\Delta x\right)\ u_{j}^{i}\geq 0\\ \left(uAC\,\big|_{j}^{i}-uAC\,\big|_{j+1}^{i}\right)/\left(A_{j}^{i}\Delta x\right)\ u_{j}^{i}<0\end{Bmatrix} \quad (11)$$

Based on the above ELFs, ICNs, and EFTCS stability condition, minimum time step Δt must be met during the numerical computations, $\Delta t = \min(\Delta t_{SWEs}, \Delta t_{ADE})$. In addition, the ADE (Eq. 3) was solved analytically for an instantaneous spill release of a mass M in grams (g) into a river in which the spill transports immediately and longitudinally along the x-axis by the advection, dispersion, and reaction processes after passing the outfall mixing zone (the spill location) as shown in Eq. 12 [9].

$$C=\frac{M}{A\sqrt{4\pi Et}}exp\ -\left[\frac{[x-ut]^{2}}{4Et}+kt\right] \quad (12)$$

2.2 Model Application

The Ohio River in the eastern United States of America, shown in Figure 3, was chosen as a field case study to build and run the developed model [10]. The river dimensions are (average length of 480000 m, average width of 800 m, and average depth of the river 10 m) with average discharge of 1500 m^3/sec. On Saturday, January 2, 1988, over 3.8 million gallons of diesel oil collapsed in a storage tank in Pittsburgh. About 800,000 gallons spilled into the river at that time. The river length was discretized using longitudinal increments (Δx) of 3001 m. The spill location is located at i = 2 and that was happened on day 2 from the start of the simulation. In addition, it was assumed that the decay rate (K) of 0.75 1/day, dispersion coefficient (E) of 700 m^2/sec, and river friction coefficient (cf) of 0.015.

In this application, the numerical model was validated by comparing the ADE numerical solution predictions ($C_{numerical}$) to the analytical solution results ($C_{analytical}$). Statistical errors such as MAE (Eq. 13) and RMSE (Eq. 14) were used to assess and evaluate model performance based on N comparisons [36,18,8,2]. Other statistics that determine the shape of the spill Gaussian plume curve such as mean (μ), standard deviation (σ), variance (σ^2), skewness (Skew), and Kurtosis (Kurt) were evaluated as shown in Eq. 15 to 18, where x_i is the value of each data point, [19,21,49].

$$MAE = \frac{\sum_1^N \left| C_{numerical} - C_{analytical} \right|}{N} \tag{13}$$

$$\mathrm{RMSE} = \sqrt{\frac{\sum_1^N \left(\mathrm{C_{numerical}} - \mathrm{C_{analytical}}\right)^2}{\mathrm{N}}} \tag{14}$$

$$\mu = \frac{1}{N}\sum_{i=1}^{N} x_i \tag{15}$$

$$\sigma = \sqrt{\frac{1}{N}\sum_{i=1}^{N} (x_i - \mu)^2} \tag{16}$$

$$Skew = \frac{1}{N}\sum_{i=1}^{N} \left[\frac{(x_i - \mu)}{\sigma}\right]^3 \tag{17}$$

$$Kurt = \frac{1}{N}\sum_{i=1}^{N} \left[\frac{(x_i - \mu)}{\sigma}\right]^4 \tag{18}$$

3. Results and Discussion

3.1 Model predictions of the instantaneous spill release by the ICNs and ELFs

The model was run using the available field data of Ohio River spill to simulate and predict the pollutant fate and transport along the river. The two

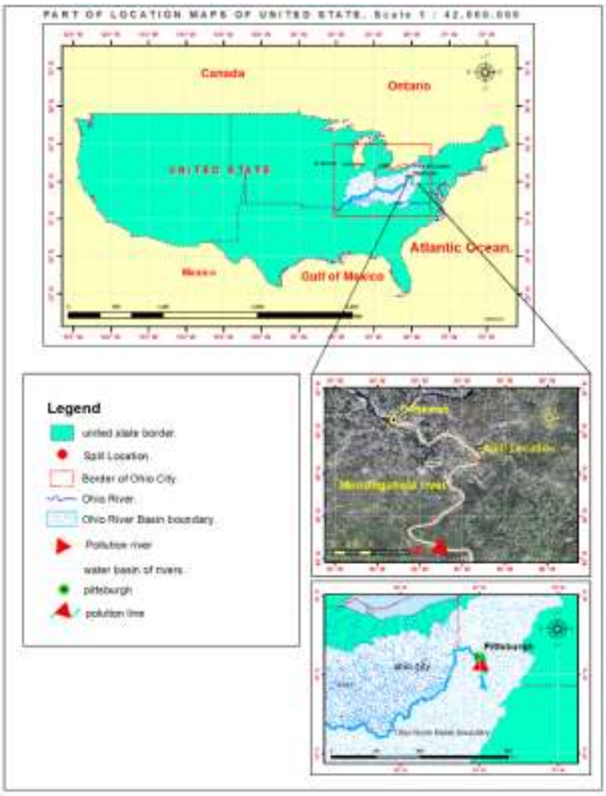

Figure 3. *Study area map: A field case study.*

numerical schemes were used for the numerical solution of SWEs. Figure 4a and 4b show the model performance results against the analytical solution for the case study presented for the Ohio River for both ICNs and ELFs, respectively, in order to verify the performance of the model. The model simulation after different times from the mass spill's start date by using both schemes reached almost the same results. When modeling the instantaneous spill release in rivers by the water quality transport equation, the most important feature of the longitudinal concentrations distribution to be predicted by the model is the leading and trailing sides of the plume concentrations compared to its peak. It is essential to predict the peak concentration because it gives information about the magnitude of the event. On the other hand, the plume sides are also important because they show how long the pollutant remains present [5]. Under the conventional (Fickian) dispersion theory, concentration measurements in space at a certain time after the release will result in a plume similar to a Gaussian bell shape.

According to the model results, the maximum concentrations occurred in the mixing zone at the outfall of the immediate spill and diminished as river distance increases. Furthermore, as travel time increases, the maximum pollutant concentration reduced as the spill mass moves downstream along the river length. For example, from 5 to 8 days, the maximum concentration predicted by the ICNs decreased from 0.1071 to 0.0084 ppm with an average flow velocity of 0.1545 m/sec (an analytical solution of a maximum concentration reduction from 0.1067 to 0.0089 ppm). On the other hand, the maximum concentration predicted by the ELFs decreased from 0.1068 to 0.0083 ppm with an average flow velocity of 0.1550 m/sec (an analytical solution of a maximum concentration reduction from 0.1066 to 0.0089 ppm). Hence, the relationship between the pollutant transport distance and time versus its concentrations is opposite as the pollution plume flows with the river length, forming a traveling bell-shaped plume of concentrations. The longer travel time and distance along the river are, the lower plume amplitude, the larger pollutant distribution [34,35]. Nevertheless, the ICNs spent higher computational time cost of about 0.5982 sec during the simulation period of 8 days, for example, while ELFs took about 0.1738 sec for the same period. This is due to the fact that the ICNs is an implicit scheme and requires solving a system of simultaneous linear algebraic equations every time level during the simulation period, while it is not for the ELFs. In addition, the ELFs skips one time step due to its numerical discretization method.

By making comparisons between the numerical solutions (ICNs and ELFs-based) and the analytical solution, there was very good agreement during the simulation times, providing good agreement with the analytical solution at the leading and trailing sides at all times. The statistical errors were very good reflecting the model robustness. The ICNs statistical errors were (RMSE: 0.0021 ppm and MAE: 0.000905 ppm) at time of 5 days and (RMSE: 0.000174 ppm and MAE: 0.0000771 ppm) at time of 8 days, while the ELFs errors were when travel time of 5 days the (RMSE: 0.0022 ppm and MAE: 0.000976 ppm) at time of 5 days (RMSE: 0.000182 ppm and MAE: 0.0000824 ppm) at time of 8 days. This reflects the model's ability to predict pollutant concentrations during different times along the river. Furthermore, Table 1 shows the plume characteristics of the pollutant concentrations distribution (Figure 4a and 4b) obtained by the model compared to the ADE analytical solution for the both SWEs schemes. Thus, it has been proven that the one-dimensional model is able to predict pollutant concentrations and agrees very well with the analytical solution.

3.2 Model predictions of the river hydrodynamics for both ICNs and ELFs

The river water level and velocity of the model predictions were compared between the ICNs and

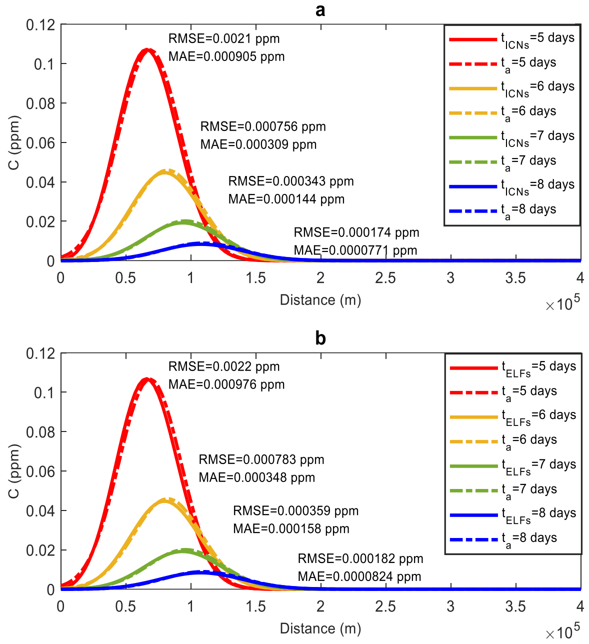

Figure 4. *Numerical model predictions compared to the analytical solution at different times (t) along the river length (Q=1500 m^3/sec, cf= 0.015, slope=0) by (a) ICNs (b) ELFs); (t_{ICNs}, t_{ELFs}, and t_a are the simulation period associated with each solution).*

ELFs. This comparison is necessary to verify the accuracy of the two schemes in balancing the height and velocity of the river water. Figure 5(a1) and 5(b1) depicts the river velocity at which the pollutant moves along the distance of the river for both schemes at the same flow condition and time. The average of velocity for the ICNs at the simulation time of 5, 6, 7, and 8 days was 0.1467, 0.1502, 0.1527, and 0.1545 m/sec, respectively, while for the ELFs the average velocity at the same times was 0.1550, 0.1507, 0.1532, and 0.1550 m/sec, respectively. Figure 5(a2) and 5(b2) displays the water levels of the river at different simulation times. The average water level at the same simulation time was 10.7194, 10.7660, 10.8006, and 10.8264 m, respectively, for the ICNs, while it was 10.7096, 10.7546, 10.7877, and 10.8123 m, respectively for the ELFs. It is clear that both schemes produced same results almost. These slight difference between the river hydrodynamics predictions of the ICNs and ELFs (Figure 5) was the divergence reason for the model pollutant concentration distribution of both schemes (Figure 4).

3.3 Model predictions sensitivity to change the grid spatial resolution

Figure 6 and 7 show the model predictions of the instantaneous spill release for both implicit and

Table 1. *Statistical summary for the plume pollutant concentrations distribution using the ICNs and ELFs compared to the analytical solution at different simulation times (t).*

ICNs statistics	t = 5 days		t = 6 days		t = 7 days		t = 8 days	
	Numerical	Analytical	Numerical	Analytical	Numerical	Analytical	Numerical	Analytical
μ (ppm)	0.0129	0.0133	0.0061	0.0063	0.0129	0.0133	0.0061	0.0063
σ (ppm)	0.0287	0.0289	0.0125	0.0129	0.0287	0.0289	0.0125	0.0129
σ^2 (ppm)	0.000825	0.000834	0.000157	0.000165	0.000825	0.000834	0.000157	0.000165
Skew	2.2399	2.1997	2.0359	2.0411	2.2399	2.1997	2.0359	2.0411
Kurt	6.6503	6.4741	5.7333	5.7644	6.6503	6.4741	5.7333	5.7644
RMSE (ppm) MAE (ppm)	0.0021 0.000905		0.000756 0.000309		0.000343 0.000144		0.000174 0.0000771	
ELFs statistics	t = 5 days		t = 6 days		t = 7 days		t = 8 days	
	Numerical	Analytical	Numerical	Analytical	Numerical	Analytical	Numerical	Analytical
μ (ppm)	0.0129	0.0132	0.0061	0.0063	0.0129	0.0132	0.0061	0.0063
σ (ppm)	0.0286	0.0288	0.0126	0.0129	0.0286	0.0288	0.0126	0.0129
σ^2 (ppm)	0.000821	0.000828	0.000158	0.000165	0.000821	0.000828	0.000158	0.000165
Skew	2.2364	2.1974	2.0333	2.0394	2.2364	2.1974	2.0333	2.0394
Kurt	6.6343	6.4633	5.7226	5.757	6.6343	6.4633	5.7226	5.757
RMSE (ppm) MAE (ppm)	0.0022 0.000976		0.000783 0.000348		0.000359 0.000158		0.000182 0.0000824	

leap-frog schemes (ICNs and ELFs), respectively, using more than one spatial resolution (Δx = 3101, 3201, and 3301 m) at different simulation times from the spill release time, (t= 5, 6, 7, and 8 days) for each resolution. Keeping other parameters constant, these resolutions were varied in which the model is stable numerically depending on the related stability condition, resulting in different time increments (Δt). By setting the fact that as the value of Δx increases, the value of Δt increases and the execution time (t_{exc}) decreases, the pollutant plume concentrations transported by the model along the river can be evaluated by comparing the model predictions of both numerical schemes with the instantaneous spill release analytical solution. This evaluation confirms the robustness of the model. As a result, the model simulation by both ICNs and ELFs depicts the numerical model stability for each spatial resolution in which the model preserves similar numerical pollutant concentrations distribution compared to the analytical solution, demonstrating that the model produces similar predictions with similar numerical behavior under different stability conditions.

Regarding the plume concentrations distribution, the both solutions were compatible at all spatial resolutions including the maximum concentration, the leading and trailing sides of the plume, see Table 2 and 3 for statistics summary of the plumes resulted by implementing the ICNs and ELFs, respectively. Very good agreement (very low RMSEs and MAEs) was achieved by both schemes compared to the analytical solution. For example, using the ICNs (Δx = 3101 and t = 5 days), the mean pollutant concentration was the same (C = 0.0128 ppm) for both solutions (numerical and analytical). As for the ELFs at the same time, the numerical solution gave (C = 0.0131 ppm), while the analytical solution was (C = 0.0132 ppm), and so on for the rest as shown in Table 2 and 3. Thus, the model was stable and gave similar values for both scheme. This numerical behavior must be held on for any numerical model to make sure that the model performance is robust. Accordingly, as long as the model obeys the numerical stability, changing the spatial grid resolution gives almost similar predictions. However, too large spatial resolution is not preferable [7,39,44].

Nevertheless, the only difference between the ICNs and ELFs is the total execution time (required to run the model. Based on the results, always the ICNs requires more computational time to run compared to the ELFs for the same input parameters.

3.4 Model Predictions Sensitivity To Change The Temporal Resolution

The model predictions of plume concentrations transported along the river were examined against the temporal increment variation for both schemes by selecting more than one value for the time step (Δt = 20, 60, and 100 sec) and keeping the other model inputs constant in which a spatial resolution value of (Δx = 3001 m) was used for both schemes so that the model is numerically stable for each Δt above. Figure 8 and 9 show the model predictions at different simulation times (t= 5, 6, 7, and 8 days) for each time increments by using the ICNs and ELFs, respectively. Hence, the numerical predictions of all times matched the analytical solution plume efficiently. Results showed that the smaller the temporal resolution is, the higher

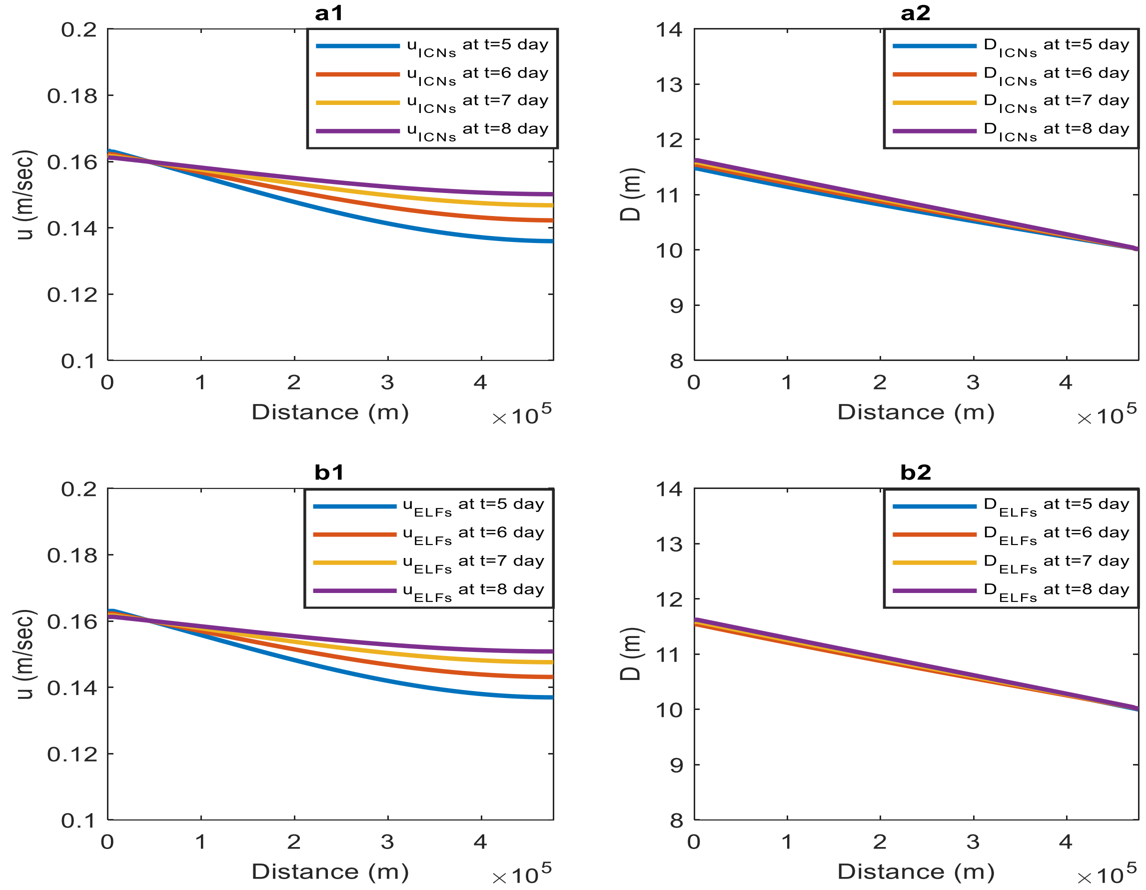

Figure 5. *Numerical solution of river hydrodynamics at different simulation times (t) along the river length ($Q=1500\ m^3/sec$, $cf= 0.015$, slope=0) by the ICNs (a1 and a2) and the ELFs (b1 and b2).*

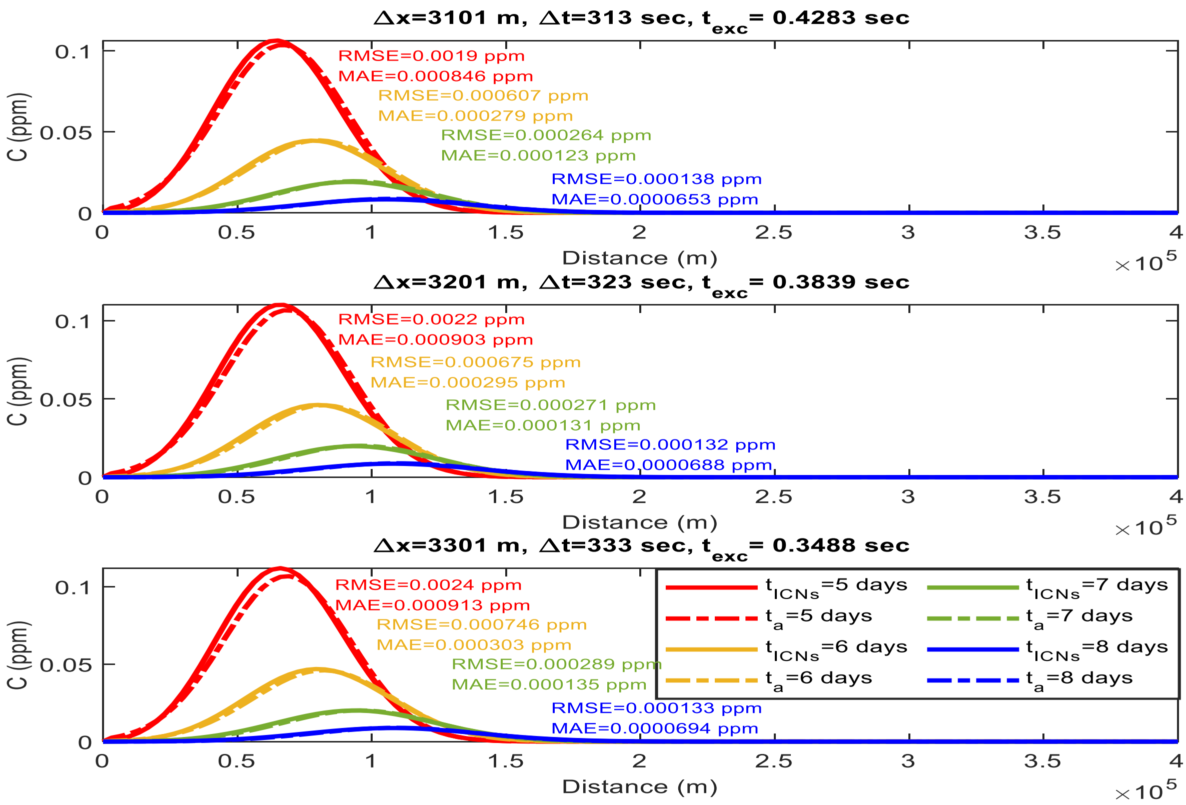

Figure 6. *Numerical model predictions at different simulation times (t) along the river length by using the ICNs with different spatial resolutions (Δx); (t_{ICNs}, t_{ELFs}, and t_a are the simulation period associated with each solution).*

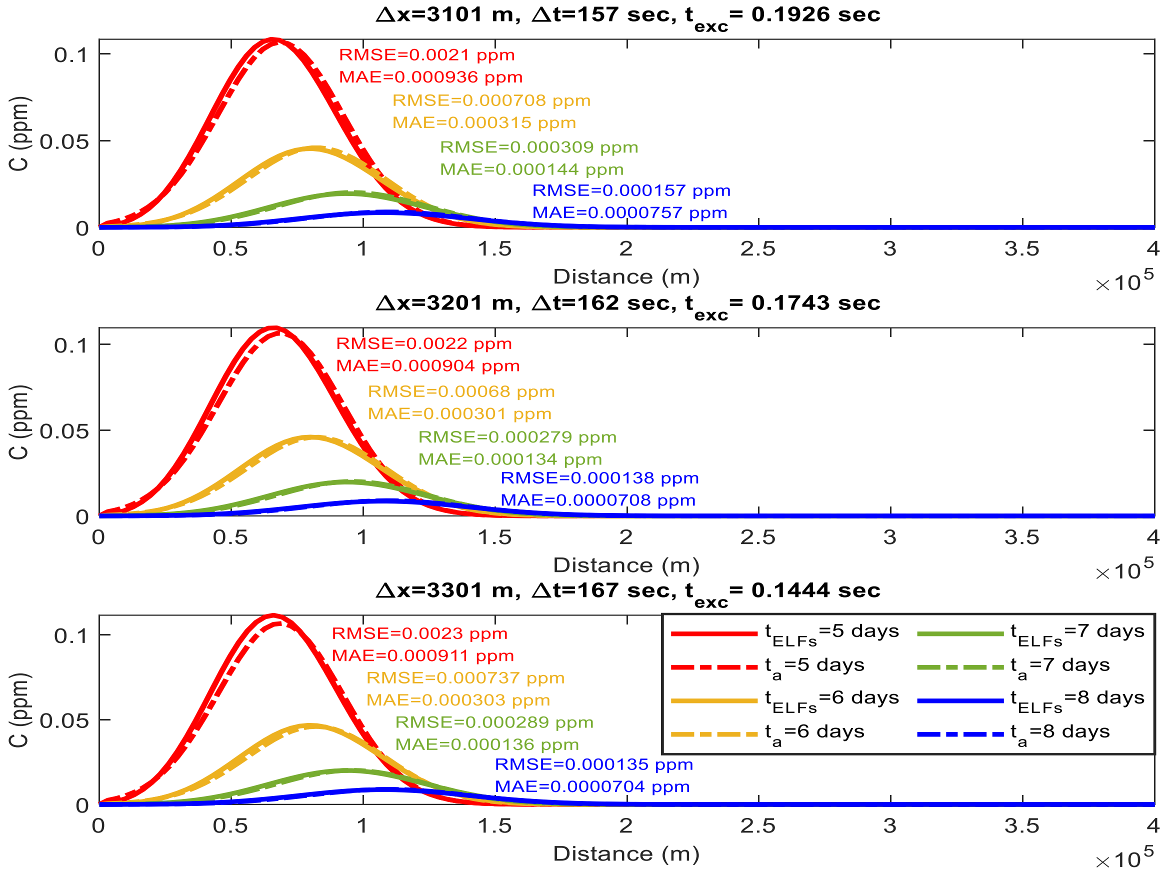

Figure 7. *Numerical model predictions at different simulation times (t) along the river length by using the ELFs with different spatial resolutions (Δx); (t_{ICNs}, t_{ELFs}, and t_a are the simulation period associated with each solution).*

Table 2. *Statistical summary using the ICNs with different spatial resolutions (Δx) for the plume pollutant concentrations distribution during different simulation times (t).*

Δx=3101 m	**t = 5 days**		**t = 6 days**		**t = 7 days**		**t = 8 days**	
	Numerical	**Analytical**	**Numerical**	**Analytical**	**Numerical**	**Analytical**	**Numerical**	**Analytical**
μ (ppm)	0.0128	0.0128	0.0061	0.0061	0.0029	0.0029	0.0014	0.0014
σ (ppm)	0.0285	0.028	0.0125	0.0125	0.0055	0.0056	0.0025	0.0026
σ^2 (ppm)	0.000812	0.000784	0.000156	0.000157	0.0000308	0.0000319	0.00000618	0.00000656
Skew	2.2455	2.1971	2.0407	2.0379	1.8786	1.9053	1.7451	1.7925
Kurt	6.6761	6.4622	5.7535	5.7503	5.0862	5.199	4.5788	4.7596
RMSE (ppm)	0.0019		0.000607		0.000264		0.000138	
MAE (ppm)	0.000846		0.000279		0.000123		0.00000653	
Δx=3201 m	**t = 5 days**		**t = 6 days**		**t = 7 days**		**t = 8 days**	
	Numerical	**Analytical**	**Numerical**	**Analytical**	**Numerical**	**Analytical**	**Numerical**	**Analytical**
μ (ppm)	0.0134	0.0132	0.0064	0.0063	0.003	0.003	0.0014	0.0014
σ (ppm)	0.0297	0.0288	0.013	0.0129	0.0058	0.0058	0.0026	0.0026
σ^2 (ppm)	0.000879	0.000829	0.000169	0.000165	0.0000335	0.0000336	0.00000673	0.00000694
Skew	2.2243	2.1988	2.0218	2.041	1.8619	1.9096	1.7302	1.7973
Kurt	6.5772	6.4699	5.6731	5.764	5.0211	5.2165	4.5248	4.7781
RMSE (ppm)	0.0022		0.000675		0.000271		0.000132	
MAE (ppm)	0.000903		0.000295		0.000131		0.0000688	
Δx=3301 m	**t = 5 days**		**t = 6 days**		**t = 7 days**		**t = 8 days**	
	Numerical	**Analytical**	**Numerical**	**Analytical**	**Numerical**	**Analytical**	**Numerical**	**Analytical**
μ (ppm)	0.0136	0.0132	0.0064	0.0062	0.0031	0.003	0.0014	0.0014
σ (ppm)	0.0301	0.0288	0.0132	0.0129	0.0059	0.0058	0.0026	0.0026
σ^2 (ppm)	0.000907	0.000829	0.000174	0.000165	0.0000344	0.0000336	0.00000693	0.00000692
Skew	2.2248	2.2058	2.0221	2.0478	1.8621	1.9162	1.7304	1.8038
Kurt	6.5794	6.5025	5.6743	5.7932	5.0219	5.243	4.5252	4.8024
RMSE (ppm)	0.0024		0.000746		0.000289		0.000133	
MAE (ppm)	0.000913		0.000303		0.000135		0.0000694	

execution time. It was observed that the model running time took (t_{exc} = 1.4054, 0.8224, and 0.6797 sec, respectively) by using the ICNs, and (t_{exc} = 0.7984, 0.3980, and 0.2126 sec, respectively) by using the ELFs. However, using a high time step in a numerically stable model does not ensure accurate results even though the stability condition is valid [51]. Therefore, it is necessary to check the model validity with different time increments within the stability range before making a decision

Table 3. *Statistical summary using the ELFs with different spatial resolutions (Δx) for the plume pollutant concentrations distribution during different simulation times (t).*

Δx=3101 m	**t = 5 days**		**t = 6 days**		**t = 7 days**		**t = 8 days**	
	Numerical	**Analytical**	**Numerical**	**Analytical**	**Numerical**	**Analytical**	**Numerical**	**Analytical**
μ (ppm)	0.0131	0.0132	0.0062	0.0063	0.0029	0.003	0.0014	0.0014
σ (ppm)	0.0291	0.0288	0.0128	0.0129	0.0057	0.0058	0.0025	0.0026
σ^2 (ppm)	0.000848	0.000829	0.000163	0.000165	0.0000322	0.0000336	0.00000647	0.00000692
Skew	2.2313	2.1985	2.0283	2.0405	1.8681	1.909	1.7362	1.7967
Kurt	6.6099	6.4685	5.7009	5.7617	5.0455	5.214	4.5466	4.7757
RMSE (ppm)	0.0021		0.000708		0.000309		0.000157	
MAE (ppm)	0.000936		0.000315		0.000144		0.00000757	
Δx=3201 m	**t = 5 days**		**t = 6 days**		**t = 7 days**		**t = 8 days**	
	Numerical	**Analytical**	**Numerical**	**Analytical**	**Numerical**	**Analytical**	**Numerical**	**Analytical**
μ (ppm)	0.0134	0.0132	0.0063	0.0063	0.003	0.003	0.0014	0.0014
σ (ppm)	0.0296	0.0288	0.0129	0.0058	0.0058	0.0058	0.0026	0.0026
σ^2 (ppm)	0.000874	0.000829	0.000168	0.000165	0.0000332	0.0000336	0.00000669	0.00000694
Skew	2.2228	2.1971	2.0203	2.0393	1.8605	1.908	1.7288	1.7957
Kurt	6.57	6.462	5.6668	5.7566	5.0154	5.2097	4.5196	4.7719
RMSE (ppm)	0.0022		0.00068		0.000279		0.000138	
MAE (ppm)	0.000904		0.000134		0.000134		0.0000708	
Δx=3301 m	**t = 5 days**		**t = 6 days**		**t = 7 days**		**t = 8 days**	
	Numerical	**Analytical**	**Numerical**	**Analytical**	**Numerical**	**Analytical**	**Numerical**	**Analytical**
μ (ppm)	0.0136	0.0132	0.0064	0.0062	0.003	0.003	0.0014	0.0014
σ (ppm)	0.03	0.0288	0.0132	0.0129	0.0059	0.0058	0.0026	0.0026
σ^2 (ppm)	0.000901	0.000829	0.000173	0.000165	0.0000342	0.0000336	0.00000689	0.00000692
Skew	2.2232	2.2041	2.0206	2.046	1.8607	1.9145	1.7289	1.8021
Kurt	6.572	6.4945	5.6679	5.7855	5.016	5.236	4.5199	4.796
RMSE (ppm)	0.0023		0.000737		0.000289		0.000135	
MAE (ppm)	0.000911		0.000303		0.000136		0.0000704	

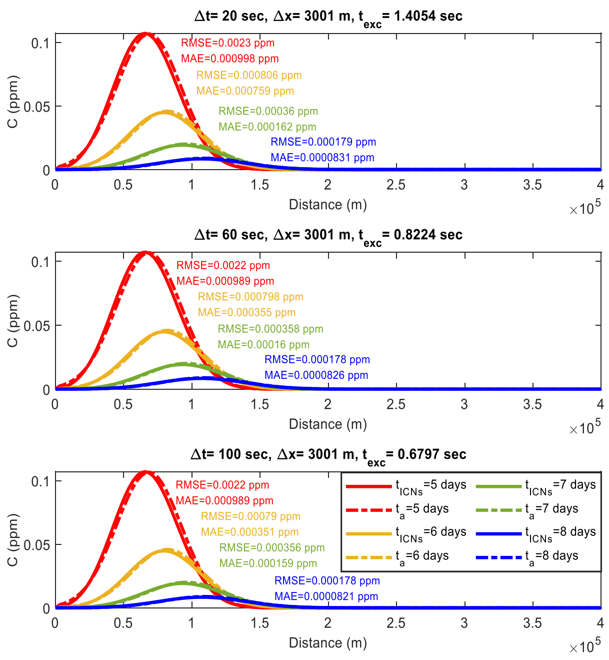

Figure 8. *Numerical model predictions at different simulation times (t) along the river length by the ICNs and different temporal resolutions (Δt); (t_{ICNs}, t_{ELFs}, and t_a are the simulation period associated with each solution).*

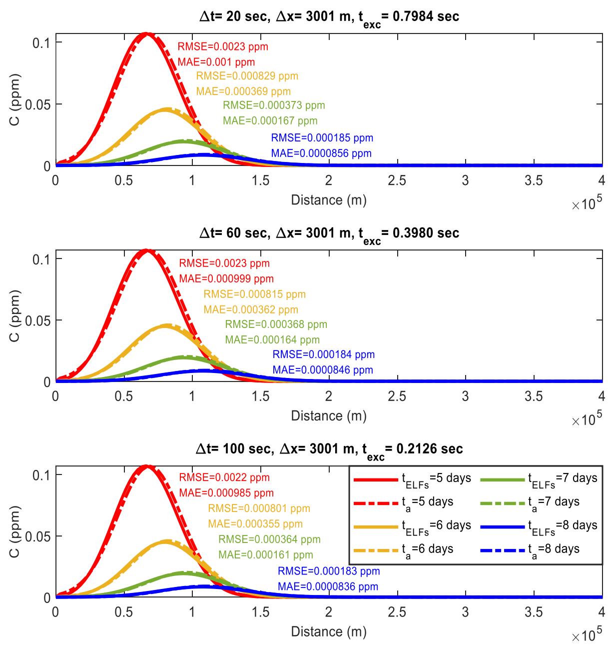

Figure 9. *Numerical model predictions at different simulation times (t) along the river length by the ELFs and different temporal resolutions (Δt); (t_{ICNs}, t_{ELFs}, and t_a are the simulation period associated with each solution).*

so that the plume concentrations conserve the pollutant mass transported along the river spatially and temporally. In addition, the plume concentrations location related to the spill location was conserved by the mode schemes along the river over time. Running the model gave similar locations for both schemes as shown in Figure 8 and 9. At t = 5 days, the plume situated at x = 69.023 m from the spill location. Likewise, the location was (x = 84.028, 96.023, and 111.037 m) at (t = 6, 7, and 8 days, respectively).

Generally, by comparing the ICNs and ELFs, you can conclude that the ELFs uses less computational time since it skips one numerical time step and eliminates the requirement to solve a linear algebraic equations system at each time step. It is also easy to implement in programming with low efforts and statistical errors. However, the two schemes are similar in that they both give almost similar robust predictions for instantaneous spill release in rivers.

4. Conclusions

In this research, a one-dimensional numerical model was built to simulate the longitudinal transport of instantaneous spills in rivers by solving the shallow water equations based on two different numerical schemes (Explicit Leap-Frog Scheme and Implicit Crank-Nicolson Scheme) and the advection-dispersion equation simultaneously. Numerical comparison was performed to highlight the effects of implementing both schemes on the pollutant concentration distribution spatially and temporally. Simulation findings of both schemes showed very good numerical robustness based on error statistics compared to the analytical solution, in which almost similar model predictions of water levels, flow velocities, and pollutant concentrations were achieved by using both schemes. Due to the Leap-Frog Scheme effects of skipping one time level and eliminating the linear algebraic equations system solution every numerical time step during the simulation period, the Leap-Frog Scheme spent less computational time cost compared to the Crank-Nicolson Scheme. Hence, lower modeling execution time and easier coding efforts are required by using the Leap-Frog Scheme. Furthermore, it is necessary to make sure that the model is valid for any applied time step even though this model is stable within its numerical stability range. Therefore, as long as the model obeys the numerical stability, changing the spatial grid resolution and using different time increments must give predictions with acceptable error statistics for water quality decision-making purposes in which the pollutant concentrations distribution along the river at any location and time conserves the transport governing equations.

Author Statements:

- **Ethical approval:** The conducted research is not related to either human or animal use.
- **Conflict of interest:** The authors declare that they have no known competing financial interests or personal relationships that could have appeared to influence the work reported in this paper
- **Acknowledgement:** The authors declare that they have nobody or no-company to acknowledge.
- **Author contributions:** The authors declare that they have equal right on this paper.
- **Funding information:** The authors declare that there is no funding to be acknowledged.
- **Data availability statement:** The data that support the findings of this study are available on request from the corresponding author. The data are not publicly available due to privacy or ethical restrictions.

References

[1] Al-Dalimy, S. Z. and Al-Zubaidi, H. A. M. (2023). One-dimensional model predictions of carbonaceous biological oxygen demand and dissolved oxygen for Hilla river water quality, Iraq. *Ecological Engineering and Environmental Technology*. 24(7). https://doi.org/10.12912/27197050/170100

[2] Al-Zubaidi, H. A. M., & Wells, S. A. (2018). Comparison of a 2D and 3D Hydrodynamic and Water Quality Model for Lake Systems. World Environmental and Water Resources Congress 2018: Watershed Management. *Irrigation and Drainage, and Water Resources Planning and Management - Selected Papers from the World Environmental and Water Resources Congress 2018*. https://doi.org/10.1061/9780784481400.007

[3] Al-Zubaidi, H. A. M., & Wells, S. A. (2020). Analytical and field verification of a 3D hydrodynamic and water quality numerical scheme based on the 2D formulation in CE-QUAL-W2. *Journal of Hydraulic Research*. 58(1). https://doi.org/10.1080/00221686.2018.1499051

[4] Andallah, L., & Khatun, M. (2020). Numerical solution of advection-diffusion equation using finite difference schemes. *Bangladesh Journal of Scientific and Industrial Research*. 55(1);15–22. https://doi.org/10.3329/bjsir.v55i1.46728

[5] Ani, E. C., Wallis, S., Kraslawski, A., & Agachi, P. S. (2009). Development, calibration and evaluation of two mathematical models for pollutant transport in a small river. *Environmental Modelling and*

Software. 24(10);1139–1152. https://doi.org/10.1016/j.envsoft.2009.03.008

[6] Ara, K. N. I., Rahaman, Md. M., & Alam, Md. S. (2021). Numerical Solution of Advection Diffusion Equation Using Semi-Discretization Scheme. *Applied Mathematics*. 12(12);1236–1247. https://doi.org/10.4236/am.2021.1212079

[7] Azad, A. K., & Andallah, L. S. (2016). Numerical Study on the Stability of Finite Differ-ence Schemes for Solving Advection Diffusion Equation. *ULAB Journal Of Science And Engineering*. 7(1).

[8] Chicco, D., Warrens, M. J., & Jurman, G. (2021). The coefficient of determination R-squared is more informative than SMAPE, MAE, MAPE, MSE and RMSE in regression analysis evaluation. *PeerJ Computer Science*. 7;1–24. https://doi.org/10.7717/PEERJ-CS.623

[9] Chin, D. A. (2006). Water-Quality Engineering in Natural Systems. *Water-Quality Engineering in Natural Systems*. https://doi.org/10.1002/0471784559

[10] Clark, R. M., Vicory, A. H., & Goodrich, J. A. (1990). The Ohio River Oil Spill: A Case Study. *Journal AWWA*. 82(3). https://doi.org/10.1002/j.1551-8833.1990.tb06934.x

[11] De Almeida, G. A. M., Bates, P., Freer, J. E., & Souvignet, M. (2012). Improving the stability of a simple formulation of the shallow water equations for 2-D flood modeling. *Water Resources Research*. 48(5). https://doi.org/10.1029/2011WR011570

[12] Delis, A. I., & Nikolos, I. K. (2021). Shallow water equations in hydraulics: Modeling, numerics and applications. *Water (Switzerland)*. 13(24). https://doi.org/10.3390/w13243598

[13] Deng, Z.-Q., Singh, V. P., Asce, F., & Bengtsson, L. (2004). Numerical Solution of Fractional Advection-Dispersion Equation. https://doi.org/10.1061/ASCE0733-94292004130:5422

[14] Durran, D. R. (1999). Numerical Methods for Wave Equations in Geophysical Fluid Dynamics. *Springer New York*. https://doi.org/10.1007/978-1-4757-3081-4

[15] El-Mikkawy, M., & Atlan, F. (2014). Algorithms for Solving Linear Systems of Equations of Tridiagonal Type via Transformations. *Applied Mathematics*. 05(03);413–422. https://doi.org/10.4236/am.2014.53042

[16] Ghane, A., Mazaheri, M., & Mohammad Vali Samani, J. (2016). Location and release time identification of pollution point source in river networks based on the Backward Probability Method. *Journal of Environmental Management*. 180;164–171. https://doi.org/10.1016/j.jenvman.2016.05.015

[17] Haltiner, G. J., and R. T. Williams, 1980: Numerical Prediction and Dynamic Meteorology. *2nd ed. Wiley*. 477. ISBN-13: 978-0471059714, ISBN-10: 0471059714

[18] Hodson, T. O. (2022). Root-mean-square error (RMSE) or mean absolute error (MAE): when to use them or not. *Geoscientific Model Development*. 15(14);5481–5487. https://doi.org/10.5194/gmd-15-5481-2022

[19] Jamalludin, D., Ahmad, A., Zakaria, Z., Hashim, M., Ibrahim, A., & Ahmad, F. (2019). Distribution of bulk unit weight of residual soils from the Northern Malaysia. *Journal of Physics: Conference Series*. 1349(1). https://doi.org/10.1088/1742-6596/1349/1/012025

[20] Keppens, R., Toth, G., Botchev, M., & Van Der Ploeg, A. (1999). Implicit And Semi-Implicit Schemes: Algorithms. *International Journal For Numerical Methods In Fluids*. 30(3); 335-352. https://doi.org/10.1002/(sici)1097-0363(19990615)30:3<335::aid-fld923>3.0.co;2-u

[21] Kohzadi, Z., Safdari, R., & Haghighi, K. S. (2021). Designing an intelligent system for diagnosing type of sleep apnea and determining its severity. *Frontiers in Health Informatics*. 10. https://doi.org/10.30699/fhi.v10i1.287

[22] Legleiter, C. J., Sansom, B. J., & Jacobson, R. B. (2022). Remote Sensing of Visible Dye Concentrations During a Tracer Experiment on a Large, Turbid River. *Water Resources Research*. 58(4). https://doi.org/10.1029/2021WR031396

[23] Li, J., & Chen, Y.-T. (2019). Computational Partial Differential Equations Using MATLAB®. *Computational Partial Differential Equations Using MATLAB®*. https://doi.org/10.1201/9780429266027

[24] Mehrmoosavi, B., Ghobadian, R., & Javn, M. (2023). Simiulation of dam break flow based on numerical solving of shallow water equations in curvilinear coordinate. *Irrigation Sciences and Engineering (JISE)*. 46(1);15–31. https://doi.org/10.22055/jise.2018.23929.1700

[25] Mesinger, F., & Arakawa, A. (1976). Numerical Methods Used In Atmospheric Models. *Global Atmospheric Research Programme (GARP) WMO - ICSU Joint Organizing Committee*. 6(17)

[26] Owowenu, E. K., Nnadozie, C. F., Akamagwuna, F., Noundou, X. S., Uku, J. E., & Odume, O. N. (2023). A critical review of environmental factors influencing the transport dynamics of microplastics in riverine systems: implications for ecological studies. *Aquatic Ecology*. 57(2);557–570). https://doi.org/10.1007/s10452-023-10029-7

[27] Panchenko, E., & Alabyan, A. (2022). Friction factor evaluation in tidal rivers and estuaries. *MethodsX*. 9. https://doi.org/10.1016/j.mex.2022.101669

[28] Parsaie, A., & Haghiabi, A. H. (2017). Computational Modeling of Pollution Transmission in Rivers. *Applied Water Science*. 7(3);1213–1222. https://doi.org/10.1007/s13201-015-0319-6

[29] Peruzzi, C., Galli, A., Chiaradia, E. A., & Masseroni, D. (2021). Evaluating longitudinal dispersion of scalars in rural channels of agro-urban environments. *Environmental Fluid Mechanics*. 21(4);925–954. https://doi.org/10.1007/s10652-021-09804-7

[30] Phosri, P., & Pochai, N. (2020). Explicit Finite Difference Techniques for a One-Dimensional Water Pollutant Dispersion Model in a Stream. *International Journal of Simulation: Systems,*

Science & Technology. https://doi.org/10.5013/ijssst.a.21.03.01

[31] Pochai, N., & Phosri, P. (2021). A Couple Mathematical Models of the Water Quality Measurement in a Stream using Upwind Implicit Methods. *IAENG International Journal of Applied Mathematics.* 51(1). https://www.iaeng.org/IJAM/issues_v51/issue_1/IJAM_51_1_27.pdf

[32] Rahaman, M. M., Andallah, L. S., & Alam, M. S. (2017). Numerical solution of advection diffusion reaction equation coupled with shallow water equation. *International Journal of Scientific & Engineering Research.* 8(11). http://www.ijser.org

[33] Rahaman, M. M., Hossain, M. J., Hossain, M. B., Galib, S. M., & Sikdar, M. M. H. (2015). Error Estimation of an Explicit Finite Difference Scheme for a Water Pollution Model. *IOSR Journal of Mathematics.* 11(4);47–61. https://doi.org/10.9790/5728-11454761

[34] Ritta, A. G. S. L., Almeida, T. R., Chacaltana, J. T. A., & Moreira, R. M. (2020). Numerical analysis of the effluent dispersion in rivers with different longitudinal diffusion coefficients. *Journal of Applied Fluid Mechanics.* 13(5);1551–1559. https://doi.org/10.36884/JAFM.13.05.31015

[35] Ramezani, M., Noori, R., Hooshyaripor, F., Deng, Z., & Sarang, A. (2019). Numerical modelling-based comparison of longitudinal dispersion coefficient formulas for solute transport in rivers. *Hydrological Sciences Journal*. 64(7).808–819. https://doi.org/10.1080/02626667.2019.1605240

[36] Robeson, S. M., & Willmott, C. J. (2023). Decomposition of the mean absolute error (MAE) into systematic and unsystematic components. *PLoS ONE.* 18(2). https://doi.org/10.1371/journal.pone.0279774

[37] Saadatpour, M., & Afshar, A. (2013). Multi Objective Simulation-Optimization Approach in Pollution Spill Response Management Model in Reservoirs. *Water Resources Management.* 27(6);1851–1865. https://doi.org/10.1007/s11269-012-0230-y

[38] Saiduzzaman, Md &, Ray, S. K. (2013). Comparison of Numerical Schemes for Shallow Water Equation. *Global Journal of Science Frontier Research Mathematics and Decision Sciences*. 13(4).

[39] Sanjaya, F., & Mungkasi, S. (2017). A simple but accurate explicit finite difference method for the advection-diffusion equation. *Journal of Physics: Conference Series.* 909(1). https://doi.org/10.1088/1742-6596/909/1/012038

[40] Sarkhosh, P., & Jin, Y. C. (2021). MPS-Based Model to Solve One-Dimensional Shallow Water Equations. *Water Resources Research*. 57(4). https://doi.org/10.1029/2020WR028742

[41] Silavwe, D. D., Brink, I. C., & Wallis, S. G. (2019). Assessment of some numerical methods for estimating the parameters of the one-dimensional advection–dispersion model. *Acta Geophysica*. 67(3);999–1016. https://doi.org/10.1007/s11600-019-00293-3

[42] Sukron, M., Habibah, U., & Hidayat, N. (2021). Numerical solution of Saint-Venant equation using Runge-Kutta fourth-order method. *Journal of Physics: Conference Series.* 1872(1). https://doi.org/10.1088/1742-6596/1872/1/012036

[43] Sun, W. Y. (2010). Instability in leapfrog and forward-backward schemes. *Monthly Weather Review.* 138(5);1497–1501. https://doi.org/10.1175/2009MWR3127.1

[44] Thongmoon, M., & Mckibbin, & R. (2006). A Comparison of Some Numerical Methods for the Advection-Diffusion Equation. *Res. Lett. Inf. Math. Sci.* 10. http://iims.massey.ac.nz/research/letters/49

[45] Timis, E. C., Cristea, V. M., & Agachi, P. S. (2015). Factors influencing pollutant transport in rivers: Fickian approach applied to the Somes river. *Revista de Chimie.* 66(9);1495-1503.

[46] Tsanis, I. K. (2007). A wind-driven hydrodynamic and pollutant transport model. *Global NEST Journal.* 9(2). https://doi.org/10.30955/gnj.000256

[47] Valiani, A., & Caleffi, V. (2024). A one-dimensional augmented Shallow Water Equations system for channels of arbitrary cross-section. *Advances in Water Resources.* 189. https://doi.org/10.1016/j.advwatres.2024.104735

[48] Vreugdenhil, C. B. (2013). Numerical methods for shallow-water flow. *Springer Science & Business Media.*

[49] Wang, X., Yang, J., Wang, F., Xu, N., Li, P., & Wang, A. (2023). Numerical Modeling of the Dispersion Characteristics of Pollutants in the Confluence Area of an Asymmetrical River. *Water (Switzerland).* 15, 3766. https://doi.org/10.3390/w15213766

[50] Welahettige, P., Vaagsaether, K., & Lie, B. (2018). A solution method for one-dimensional shallow water equations using flux limiter centered scheme for open Venturi channels. *Journal of Computational Multiphase Flows.* 10(4);228–238. https://doi.org/10.1177/1757482X18791895

[51] Wells, S. A. (2002). Basis for the CE-QUAL-W2 version 3 river basin hydrodynamic and water quality model. *ASCE International Water Resources Engineering Conference. https://pdxscholar.library.pdx.edu/cgi/viewcontent.cgi?article=1112&context=cengin_fac*

[52] Wu, J., & Yu, X. (2021). Numerical investigation of dissolved oxygen transportation through a coupled swe and streeter-phelps model. *Mathematical Problems in Engineering*. 2021. https://doi.org/10.1155/2021/6663696

[53] Xia, X., & Liang, Q. (2018). A new efficient implicit scheme for discretising the stiff friction terms in the shallow water equations. *Advances in Water Resources.* 117;87–97. https://doi.org/10.1016/j.advwatres.2018.05.004

[54] Yan, B., Liu, Y., Gao, Z., & Liu, D. (2022). Simulation of Sudden Water Pollution Accidents in Hunhe River Basin Upstream of Dahuofang Reservoir. *Water (Switzerland).* 14(6). https://doi.org/10.3390/w14060925

[55] Yarodji, M. A. K., Badé, R., & Saley, B. (2020). Study of the 1D Saint-Venant Equations and

Application to the Simulation of a Flood Problem. *Journal of Applied Mathematics and Physics*. 08(07);1193–1206. https://doi.org/10.4236/jamp.2020.87090

[56] Yip, B. F., Alias, N. A. F., & Kasiman, E. H. (2021). Numerical Modelling of Pollutant Transport in a Straight Narrow Channel using Upwind Finite Difference Method. *IOP Conference Series: Materials Science and Engineering*, 1153(1), 012003. https://doi.org/10.1088/1757-899x/1153/1/012003

[57] Zeunert, S., & Meon, G. (2020). Influence of the spatial and temporal monitoring design on the identification of an instantaneous pollutant release in a river. *Advances in Water Resources.* 146. https://doi.org/10.1016/j.advwatres.2020.103788

[58] Zhou, J., Bao, W., Li, Y., Cheng, L., & Bao, M. (2018). The modified one-dimensional hydrodynamic model based on the extended Chezy formula. *Water (Switzerland).* 10(12). https://doi.org/10.3390/w10121743